Electron spin changes during general anesthesia in *Drosophila*

Luca Turin[a,1], Efthimios M. C. Skoulakis[a], and Andrew P. Horsfield[b]

[a]Division of Neuroscience, Biomedical Sciences Research Centre Alexander Fleming, 16672 Vari, Greece; and [b]Department of Materials, Imperial College London, London SW7 2AZ, United Kingdom

Edited* by Mark A. Ratner, Northwestern University, Evanston, IL, and approved July 15, 2014 (received for review March 10, 2014)

We show that the general anesthetics xenon, sulfur hexafluoride, nitrous oxide, and chloroform cause rapid increases of different magnitude and time course in the electron spin content of *Drosophila*. With the exception of $CHCl_3$, these changes are reversible. Anesthetic-resistant mutant strains of *Drosophila* exhibit a different pattern of spin responses to anesthetic. In two such mutants, the spin response to $CHCl_3$ is absent. We propose that these spin changes are caused by perturbation of the electronic structure of proteins by general anesthetics. Using density functional theory, we show that general anesthetics perturb and extend the highest occupied molecular orbital of a nine-residue α-helix. The calculated perturbations are qualitatively in accord with the Meyer–Overton relationship and some of its exceptions. We conclude that there may be a connection between spin, electron currents in cells, and the functioning of the nervous system.

General anesthesia (GA) is both indispensable and fascinating. Millions of surgical procedures are performed each year, most of which would be unthinkable if GAs did not exist. However, although the first clinical anesthesia with diethyl ether was reported over 160 y ago (1), the mechanism by which the same GAs act on animals as far apart in evolution as paramecia and man (2)—and even plants (3–5)—is still unclear. In 2005, GA was included in a *Science* list of major unsolved problems in the august company of cancer, quantum gravity, and high-temperature superconductivity (6). Today, GA remains an intellectual challenge and arguably, one of the few experimental inroads to consciousness (7–9).

The mystery of GA resides in a uniquely baffling structure–activity relationship: the range of compounds capable of acting as GAs makes no pharmacological sense. Adrien Albert (10) called it "biological activity unrelated to structure" (10). In number of atoms, the simplest of the GAs is xenon (11, 12), a monoatomic noble gas, and the most complex is alfaxalone (3-hydroxypregnane-11,20-dione), a 56-atom steroid (13), spanning a 35-fold range in molecular volume. In between is a host of molecules of widely different structures: nitrous oxide, halogenated compounds [sulfur hexafluoride (SF_6), chloroform, halothane, etc.], strained alkanes (cyclopropane), phenols (propofol) (14), ethers (diethyl ether and sevoflurane), amides (urethane), sulfones (tetronal), pyrimidines (barbiturates), etc. If one adds gases, like dioxygen and nitrogen, that cause narcosis under pressure and volatile solvents used as inhalational recreational drugs, the list is longer still. What property can all these molecules possibly have in common that causes GA?

A partial answer has been known for nearly a century. GAs are lipid-soluble, and their potency, regardless of structure, is approximately proportional to lipid solubility [with some exceptions (15)], a relationship known as the Meyer–Overton rule (16, 17) that is reviewed in ref. 1. This relationship implies, surprisingly in light of their diverse structures, that, after they have arrived at their destination, all GAs are equally effective. Accordingly, because GAs dissolve in the oily core of the lipid bilayer, they were long thought to perturb the featureless dielectric in which ion channels, receptors, and pumps are embedded (18–24), although an action on proteins could never be ruled out (25, 26). Other theories were also proposed, involving the formation of gas hydrates (27), proton leaks (28), hydrogen bonds (29, 30), and membrane dipoles (31). In the 1980s, however, after the discovery of an effect of anesthetics on firefly luciferase (32), Franks and Lieb (33) first showed enzyme inhibition by GAs (34) and then differences in potency between GAs enantiomers (35, 36). This finding pointed to a protein site of action, likely a weakly chiral hydrophobic pocket (37–39). Indeed, GAs are now believed to act on proteins (40–42) and have now been seen in just such sites in protein structures, where they exert small but definite effects on protein (43) and ion channel (44) conformation. The Meyer–Overton rule then becomes all the more surprising, because protein binding sites are usually highly selective for ligand shape and size.

However, if, indeed, both the Meyer–Overton rule and the Franks–Lieb protein hypothesis are taken to be correct, a single mechanism should be shared by all GAs at the protein binding site(s). Then, the small GAs, especially xenon, drastically constrain the range of possibility. Xenon is uniquely slippery and falls outside the normal confines of molecular recognition. It has no shape, because it is a perfect sphere of electron density. It has no chemistry either at any rate under conditions found in the brain. However, and this is the hitherto overlooked starting point of the ideas developed in this paper, xenon has physics: like many other elements and molecules, it is capable of facilitating electron transfer between conductors: recall the iconic photograph of the IBM logo written in Xe atoms in a scanning tunneling microscope (STM) (45). Each Xe atom is a bump, because it facilitates tunneling from substrate to tip, and the tip must rise above it to keep the current constant (46). Indeed, among the many molecules that have been imaged in the STM are several GAs or close congeners other than xenon: nitrous oxide (47),

Significance

One hundred sixty years after its discovery, the molecular mechanism of general anesthesia remains a notable mystery. A very wide range of agents ranging from the element xenon to steroids can act as general anesthetics on all animals from protozoa to man, suggesting that a basic cellular mechanism is involved. In this paper, we show that volatile general anesthetics cause large changes in electron spin in *Drosophila* fruit flies and that the spin responses are different in anesthesia-resistant mutants. We propose that anesthetics perturb electron currents in cells and describe electronic structure calculations on anesthetic–protein interactions that are consistent with this mechanism and account for hitherto unexplained features of general anesthetic pharmacology.

Author contributions: L.T. and E.M.C.S. designed the fly experiments; L.T. and A.P.H. designed the density functional theory calculations; L.T. performed experiments and calculations; and L.T., E.M.C.S., and A.P.H. analyzed data and wrote the paper.

The authors declare no conflict of interest.

*This Direct Submission article had a prearranged editor.

Freely available online through the PNAS open access option.

[1]To whom correspondence should be addressed. Email: lucaturin@me.com.

www.pnas.org/cgi/doi/10.1073/pnas.1404387111

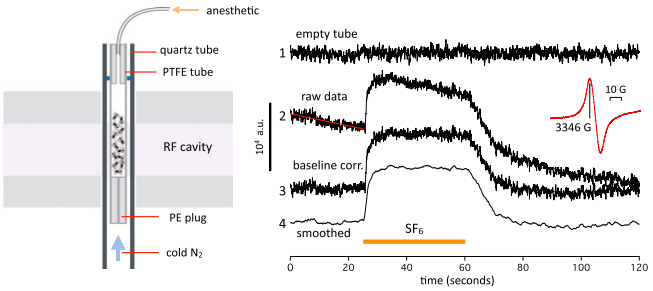

Fig. 1. (*Left*) Experimental setup for continuous spin measurements on live flies; ~28–32 *Drosophila* are housed in a polytetrafluoroethylene tube inserted into a quartz tube and positioned in the RF resonator cavity of an ESR spectrometer. A hollow polyethylene plug at the bottom allows the temperature-controlled cooling gas coming up from below (blue arrow) to enter the fly tube if the other end is left open. Anesthetics are introduced in the chamber by connecting a syringe to the top plug and cannula. The total chamber volume is about 1.5 mL. (*Right*) Continuous measurements of spin at a fixed value of magnetic field corresponding to the peak of the intrinsic spin resonance (*Inset*). In each 2-min trace, the sample chamber is filled with SF_6 for 36 s from the 24-s time mark. At other times, temperature-controlled nitrogen at 6 °C flows through the chamber. Trace 1, empty chamber (signal unaffected by SF_6); traces 2–4, recording from W1118 WT flies. The raw data (trace 2) are baseline-corrected (baseline corr.) by fitting a straight line to the period before SF_6 exposure and subtracting that line from the entire trace, yielding trace 3. Trace 3 is then smoothed with a 50-point box filter (trace length is 4,096 points) to remove instrumental high-frequency noise. Note that the noise level is highest in the empty chamber.

phenols (48), ethers (49), benzene (50), amides (51), and pyrimidines (52).

Suppose then that there exists, in one or more proteins essential to CNS function, a hydrophobic site lined with an electron donor on one side and an acceptor on the other side. When GAs enter the site, they could connect donor to acceptor by creating a pathway for electron transfer where there was no pathway. Indeed, our calculations show that, for example, xenon can extend the highest occupied molecular orbital (HOMO) of an α-helix in such a way as to bridge the gap to another helix (see Fig. 10). This spread, in proteins as well as the STM, is expected to be such a general property of molecules that if a connection were found between it and anesthesia, the Meyer–Overton rule would follow naturally. How would one detect these electron currents in a whole organism? If the electrons were unpaired, ESR would provide a specific, although not particularly sensitive, detection method, the only one presently applicable to whole animals. It, therefore, seemed interesting to ask whether one could detect changes in electron spin during anesthesia.

Methods

***Drosophila*.** *Drosophila* were cultured in standard wheat flour sugar food (53) supplemented with soy flour and $CaCl_2$ at 20–22 °C.

ESR Measurements. An Adani EMS 8400 (www.adani.by) fitted with a temperature control attachment was used to measure spin in live flies. The flies were paralyzed briefly with CO_2, and ~30 flies were dropped into a Teflon tube with a 3.5-mm i.d. (Fig. 1, *Left*). The tube was placed in the radio-frequency (RF) cavity. RF parameters were frequency ~9.4 GHz, 90 mW, and 6 dB attenuation. Measurements at attenuations between 3 and 21 dB showed an approximately linear relationship to the square root of incident RF power and no evidence of saturation. The magnetic field was modulated at 1,000 μT. Fixed magnetic field recordings were sampled at 34.13 samples/s for 120 s. The time constant of the ESR detector circuit is ~10 ms. Magnetic field scans were done at 24 s/mT. Except where otherwise specified, the flies were kept at 6°C to immobilize them. The flies were bathed in a stream of temperature-controlled nitrogen flowing from below with a pressure into the tube of 6 mbar. The experiments typically lasted less than 30 min, after which control flies not exposed to anesthetics invariably revived rapidly. An approximate (54) calibration of the ESR was performed by wetting a small piece of filter paper with 20 μL solution of 1 μM 1-λ_1-oxidanyl-2,2,6,6-tetramethylpiperidin-4-ol in water. The amplitude of the calibration signal was ~3,000 arbitrary units at the gain settings used in the continuous measurements reported in this paper. The data were processed with LabView (www.ni.com) and plotted with Igor (www.wavemetrics.com).

Density Functional Theory Calculations. The Amsterdam Density Functional (ADF) (www.scm.com) density functional theory (DFT) package was used in the calculations. All structures were optimized using the Perdew–Burke–Ernzerhof functional and core double zeta, valence triple zeta, polarized basis set (TZP) (helix alone) or a dispersion-corrected PBE-D3 functional and TZP basis set (helix and anesthetic). Orbitals were then recalculated at the final geometry using B3LYP-TZP. Some semiempirical preoptimizations as well as orbital volume calculations were performed in MacSpartan 14 (www.wavefun.com). Calculations were done on a 12-core Apple MacPro.

Results

ESR Measurements in *Drosophila*. Organic free radicals are so reactive that their concentration in living cells is generally found to be subnanomolar and therefore, unmeasurable by ESR, which has a detection limit that is approximately three orders of magnitude higher (55). In the absence of spin traps, which integrate the free radical signal over time, the cellular component contributing most of the free electron spin signal (i.e., with a g factor near 2.0) will be melanins, which typically contain 10^{18} spins/g (56). Flies are heavily pigmented, and we can expect a melanin signal proportional to pigmentation. This is the case, as shown in ref. 57, and it was replicated with our equipment in Fig. 2, *Right*, *Inset*. Three strains of *Drosophila*, namely normally pigmented WT, yellow-white, and red-eyed but yellow-bodied upstream activating sequence-neuralized (the latter two are devoid of eumelanin but still contain pheo- and neuromelanins), exhibit spin signals proportional to pigmentation. The melanin signal is unremarkable and centered around 2.0 with a width of ~10 G (Fig. 1, *Right*, *Inset*). No spin traps were used in these experiments.

Spin increases reversibly during exposure to the GA SF_6. Against this large but on a scale of minutes presumably steady melanin background, we seek a signal that varies with anesthesia. As a first guess, we expect it to also be around $g = 2.0$ but likely be

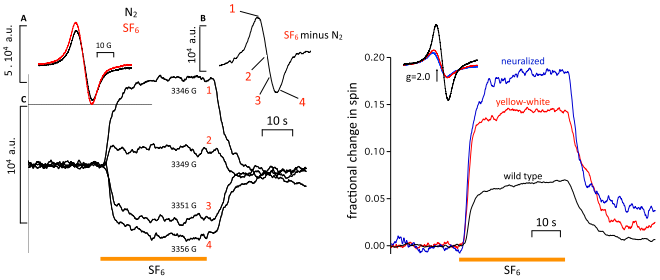

Fig. 2. (*Left*, *Inset A*) Spin signal from ~30 W1118 WT flies before (black trace) and after (red trace) exposure to SF_6. (*Left*, *Inset B*) Difference trace resulting from the two traces in *Left*, *Inset A* (i.e., the spin signal introduced by SF_6). (*Left*, *Inset C*) Four traces measured at fixed values of magnetic field corresponding to points 1–4 on trace B (i.e., 1, near the top; 2, close to the cross-over; 3, halfway down; 4, just past the bottom peak). The amplitude of the traces in *Left*, *Inset C* matches the amplitudes expected from *Left*, *Inset B*, showing that the spin changes seen in fixed field continuous measurements do, indeed, reflect an underlying resonance. The other anesthetics behave similarly. (*Right*) Effect of melanin content in different fly strains on anesthetic-induced spin changes. (*Inset*) Intrinsic spin signals of W1118 WT and two pale fly strains [yellow-white (red trace) and neuralized (blue trace)] in which eumelanin is absent. The intrinsic spin signal of the pale strains is much smaller, which was expected. Percentage change in spin in response to SF_6 in the three strains. If the signal was caused by melanin, it should either be reduced in amplitude or disappear altogether. Instead, it increases in inverse proportion to the intrinsic spin level, showing that the two are independent.

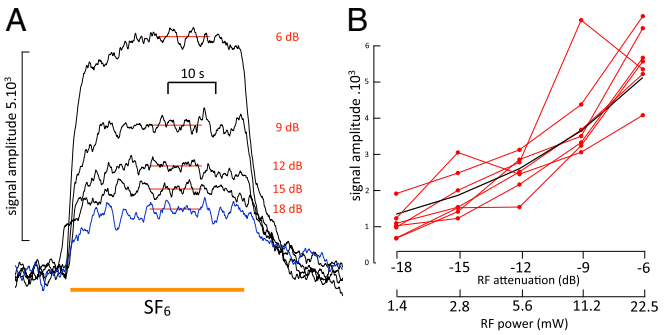

Fig. 3. (*A*) Effect of variations in incident RF power on the amplitude of the SF_6-induced spin change. Note that the onset shows a small step change even at the higher attenuations, which is probably caused by a transient temperature increase of the preparation briefly exposed to room temperature SF_6 gas until the latter cools to 6 °C. The 18-dB trace is shown in blue to facilitate comparison of onset and end. Amplitude measurements were accordingly made by subtracting the signal after recovery from the average value of the signal during a steady-state period during exposure, which is indicated by the red horizontal bars in the traces. (*B*) SF_6 signal amplitude as a function of RF power in seven different experiments (red lines). The black trace is the expected relationship if the signal is proportional to the square root of power. A signal value of 5,000 at 6 dB was chosen to position the calculated curve amid the experimental data.

much smaller than the melanin signal. We, therefore, made high-sensitivity measurements at a fixed value of magnetic field corresponding to the positive peak of the background spin signal (i.e., ~3,340 G; the exact value varies slightly from experiment to experiment and is set each time).

Fig. 1 shows a typical experiment illustrating spin changes during exposure to SF_6, a chemically inert anesthetic gas that was found to give the largest signal (*Amplitude and time course of spin changes depend on the anesthetic* discusses effects of other anesthetics). The duration of a single trace (4,096 points) is 120 s. Here, ~30 flies are measured continuously in a fixed magnetic field of 3,346 G. The flies are initially bathed in nitrogen at 6 °C. The low temperature is necessary to make sure that the flies do not move, which would make the measurements impossible. At t = 24 s, SF_6 gas is injected into the chamber. The spin signal increases rapidly and stabilizes at a new value ~7,000 units higher. At t = 60 s, N_2 is readmitted to the chamber, and the signal returns to baseline with a slower time course than that of the onset. The raw data (Fig. 1, *Right*, trace 2) are baseline-corrected by fitting a line to the period immediately preceding exposure to the anesthetic and subtracting the line from the signal (Fig. 1, *Right*, trace 3); the signal is then low-pass filtered by box-averaging (50 points) (Fig. 1, *Right*, trace 4). An empty chamber (Fig. 1, *Right*, trace 1) gives no signal and slightly more noise than when flies are present. The noise, therefore, seems to be largely instrumental in origin and is, at high frequencies, compared with those of the signal.

Anesthetic-induced spin change is a resonance. To check that the anesthetic-induced spin change is not caused by a change in baseline because of either a broad background resonance or a mistuning of the RF cavity, we exposed the flies successively to SF_6 at values of the magnetic field close to the peak, the cross-over point and the trough of the background signal. A resonance centered around 2.0 should be positive at the peak, near 0 near crossover, and negative in the trough. Fig. 2, *Left* shows that it is the case. Exposures to SF_6 at 3,346, 3,349, and 3,356 G give signals that are positive, close to zero, and negative, respectively. Accordingly, subtracting the background spin signal (Fig. 2, *Left*, *Inset A*, black trace) from the spin during SF_6 exposure (Fig. 2, *Left*, *Inset A*, red trace) yields a clearly resonant signal, with amplitude that matches well the traces taken at the different magnetic fields. Responses to other anesthetics (see below) exhibit the same sign reversal when measured in the trough. We conclude that the spin change caused by SF_6 exposure is a genuine spin resonance. A typical SF_6 signal of 7,000 units, therefore, represents an increase in spins in the cavity of the order of 2.8×10^{13} spins.

SF_6-induced spin change is independent of eumelanin content. There are many yellow *Drosophila* strains in which eumelanin is absent. We used two strains: yellow-white and neuralized. As expected from previous work (57), the background spin signal in yellow-white and neuralized is reduced to about one-third of the WT spin signal (Fig. 3*B*). The change in spin during exposure to SF_6, however, does not scale with the eumelanin content but instead, becomes proportionately larger as total spin is reduced in the yellow mutants, suggesting that it is not caused by eumelanin. We cannot rule out that the spin signal reflects an increase in the spin of pheo- or neuromelanin, because we have, to date, been unable to obtain strains of completely amelanistic flies.

Properties of the SF_6-induced spin signal. The measurements above were made with a large modulation depth of 10 G to maximize signal amplitude. This signal size is achieved at the expense of line-shape resolution. To measure line shape optimally, we first determined the relationship between microwave power and amplitude of the SF_6-induced signal. The background melanin signal was previously shown not to be near saturation (*Methods*). Here, we check for the power–intensity relationship of the additional anesthetic-induced spin. The results are shown in Fig. 3*A*. Repeated exposures to SF_6 at different power settings ranging from −6 (22.5 mW RF incident power) to −18 dB (1.4 mW RF) showed a monotonic relation between signal amplitude and RF power. The results of seven such experiments done in both WT and yellow-white strains are shown in Fig. 3*B*. They agree reasonably well with the predicted power–signal relationship far from saturation, namely a signal proportional to the square root of incident power. Measurements made at 6 dB were highly repeatable over a scale of tens of minutes, whereas at higher power, values (3 dB and above) showed some instability and increase in noise. It is not clear whether this noise increase is because of the flies warming up enough to move or the heating being sufficient to cause damage.

To measure line shape, a modulation depth of 2 G was chosen, because it seemed to be the largest value consistent with no distortion of underlying line width. However, signal-to-noise

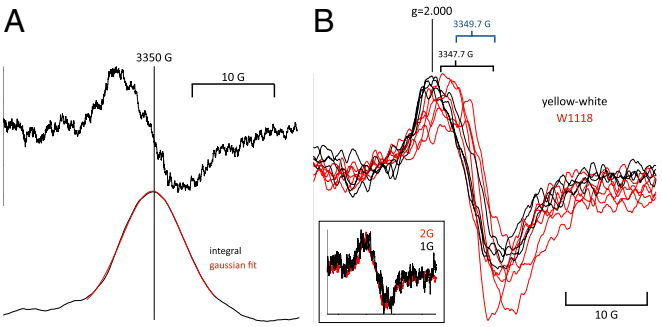

Fig. 4. (*A*, *Upper*) The SF_6-induced spin signal obtained by subtracting averaged signals from 20 sweeps in N2 from the same in SF_6. (*A*, *Lower*) The same signal integrated to show the shape of the absorption line. The red line fit to the central section of the signal is a Gaussian curve with an SD of 5.2 G. (*B*, *Inset*) Line shape of the SF_6-induced spin change measured at 2- and 1-G modulation depth. The 1-G trace is noisier, but the line shape is unchanged, showing that measurements at 2-G modulation do not distort it. Superimposed traces from five WT (red) and four yellow-white (black) experiments showing that, despite some variation in both amplitude and midpoint magnetic field value, the signals are of similar shape and show no obvious features attributable to hyperfine structure.

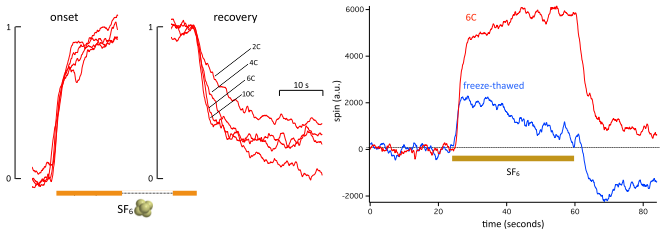

Fig. 5. Effect of temperature on (*Left*) onset and (*Center*) recovery from an SF_6 exposure. Traces have been normalized and time-adjusted to match start and end points of anesthetic onset. The ESR chamber was kept at 2 °C, 3 °C, 6 °C, and 10 °C. The onset traces are very similar and show no temperature effect. The recovery traces show a marked temperature effect (three experiments). (*Right*) Effect of freeze–thaw on the SF_6-induced spin change. The red trace is the control trace at 6 °C, and the blue trace is the same preparation 7 min later after being cooled to −130 °C and brought back immediately to 6 °C. The SF_6-induced spin change is reduced to less than one-half of its original amplitude, and it is now transient rather than steady (three experiments).

ratio was poor, and 20 sweeps were averaged in N_2 and SF_6 before being subtracted. The results are shown in Fig. 4. In Fig. 4*A*, a single unsmoothed trace (taken from the same experiment as in Fig. 3*A*) is shown together with its integral, showing that the line shape is well-fitted by a Gaussian curve. Coincidentally, this was the experiment that gave the best fit to a Gaussian curve. Records from other experiments are shown at right after smoothing. When integrated, they were about equally well-fitted by Lorentzian and Gaussian curves, suggesting that the relaxation is fast enough to prevent saturation but not fast enough to achieve a pure Lorentzian line shape. The magnetic field value at the turnover point has a range of about 2 G, and the amplitudes and line shapes are very similar in both yellow-white and WT flies (i.e., ∼10-G width at maximum slope). No additional lines or repeatable features consistent with hyperfine structure are visible.

SF_6 spin change recovery is temperature-dependent, and onset is not. We measured the SF_6-induced change in spin at different temperatures within the range of temperatures that we could explore without causing the flies to wake up and move, namely 2–10 °C. Recordings at temperatures higher than 10 °C tend, with time, to become noisy and less stable. The onset is unaffected by temperature, whereas the recovery usually changes markedly, becoming much faster at higher temperatures. However, the recovery does not follow a single exponential fit. Even after filtering, the traces are too noisy to make a multiexponential fit meaningful. Qualitatively, however, the time to full recovery at 10 °C in the experiment shown in Fig. 4 is at least five times shorter than at 2 °C. The amplitude of the signal, however, seems to be smaller at higher temperatures, decreasing by about one-half between 2 °C and 10 °C. There is considerable variability in these experiments, the origin of which is unclear considering that isogenic flies of the same strain are used every time.

SF_6-dependent spin signal requires cell integrity. Because the temperature dependence indicates a possible connection with cell metabolism, it seemed interesting to ask whether the signal also requires cell integrity. A straightforward way to test is to freeze–thaw the flies. A thermostat maintains the flies below room temperature by heating a flow of nitrogen with inlet temperature that is ∼−140 °C. When the heater is turned off, the flies reach −130 °C in ∼3 min, and an equivalent time is required to bring them back to 6 °C. Such a freeze–thaw cycle is a commonly used technique to prepare cell lysates (58). The SF_6-induced change in spin is profoundly altered by the freeze–thaw cycle (Fig. 5, *Right*): its amplitude is reduced to about one-half of the initial signal, and the time course is now transient. We conclude that cell integrity is required for the SF_6-induced change in spin. This experiment also serves as a control for the possibility that SF_6 dissolved in the flies, despite having no dipole moment, could somehow perturb the tuning of the RF cavity. In the 7 min that it takes to go from 6 °C to −130 °C and back, it is very unlikely that the flies' ability to adsorb SF_6 will have changed. However, the signal is very different.

Amplitude and time course of spin changes depend on the anesthetic. If W1118 WT flies are exposed successively to different GAs, a spectrum of responses is seen. In Fig. 6, the traces were obtained in the order Xe, SF_6, N_2O, and $CHCl_3$. Almost no response is seen to N_2O, a small and slow response is seen to Xe, the normal response is seen to SF_6, and an essentially irreversible response is seen to $CHCl_3$. Because the chloroform vapor is taken from a large bottle open to air, the flies are bathed in air briefly before the chloroform exposure. This exposure to dioxygen causes a spin change (the dioxygen signal), which is discussed further in *Spin responses differ in anesthetic-resistant mutants*.

These experiments are done in conditions that are unphysiologic but necessary to reveal the effects of maximal concentrations of anesthetic gases on the preparation against as quiet a background as possible. First, the flies are kept at 6 °C to avoid movement artifacts. Second, to maximize gas concentrations and isolate the effect of each gas from that of oxygen, the gases are pure. Consequently, the flies are kept anoxic for the duration of the experiment, except immediately before and during chloroform exposure. This hypoxia is known to cause no lasting damage (59), and indeed, four strains recover fully when in air at room temperature after the full series of anesthetics. We plan in additional experiments to explore the effects of gas mixtures containing oxygen. Third, of four anesthetics used, only chloroform causes complete anesthesia. It would be interesting to extend these measurements to ether, a potent *Drosophila* anesthetic. Unfortunately, all ethers—diethyl ether itself, fluorinated alkyl ethers, such as sevoflurane, and the convulsant ether fluothyl—perturb the ESR signal, even with an empty chamber, to such an extent that measurements are impossible. We surmise that this perturbation may be caused by the large dipole moment of ethers, which causes RF absorption around the working frequency of the X-band spectrometer (9.4 GHz) (60). The other

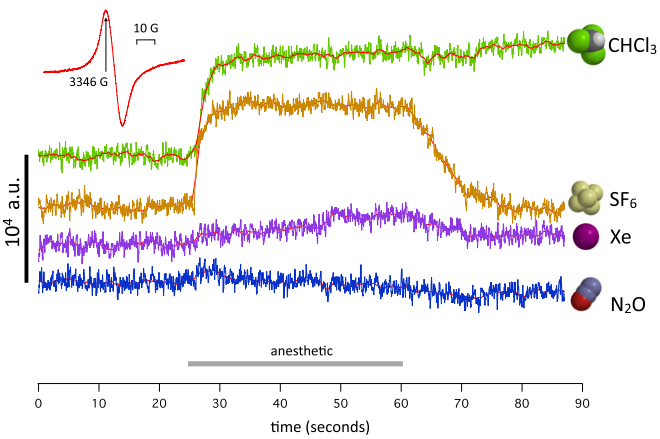

Fig. 6. Four traces of continuous measurements of spin at a fixed value of magnetic field corresponding to the peak of the intrinsic spin signal (*Inset*; 3,346 G). The traces are obtained in sequence on the same batch of W1118 WT flies kept at 6 °C and bathed in nitrogen gas. The order of exposure was Xe, SF_6, N_2O, and $CHCl_3$. The colored traces represent baseline-corrected raw data from the spectrometer. The red traces are the same after smoothing with a 50-point box filter. No signal is present in nitrous oxide, and a small signal is present in xenon. The sulfur hexafluoride and chloroform signals have a similar amplitude, but the chloroform signal seems irreversible on this time scale.

gases used were checked for artifacts like in Fig. 1, *Right*, trace 1 and found to give no spurious signal. Note that monoatomic Xe, homonuclear O_2 and N_2, and centrosymmetric SF_6 have no dipole moment and therefore, do not absorb microwaves at all. (Oxygen is a paramagnetic ground-state triplet and therefore, does absorb microwaves when placed in a magnetic field, but the signal is too broad to be detected in these experimental conditions.)

Spin responses differ in anesthetic-resistant mutants. The changes in the total ESR signal caused by GAs described so far on WT flies are suggestive but not conclusive. Anesthetics perturb a host of other biochemical processes, some of them obviously electrochemical-like respiration. One cannot, therefore, assert from measurements on WT flies alone that a causal connection exists between change in spin on the one hand and anesthesia on the other hand. However, the availability of anesthetic-resistant mutants of *Drosophila* provides an elegant way out of this needle-in-a-haystack problem. These remarkable mutants are selected by subjecting large populations of flies to a chromatography, in which only flies that stay awake in anesthetic gas cling to the stationary phase, whereas the others are eluted (61–64). We used six such mutants: one was HAR85, where the mutation has been shown to affect an ion channel (65). The others were autosomal gene anesthetic-resistant (AGAR) mutants isolated by Madhavan et al. (64), who supplied us with the stocks. They were AGAR11, -21, -52, -53, and -211. The genes affected by these mutations have not been identified.

The results are shown in Fig. 7. Because there is some variability from experiment to experiment on the same strain of flies, the traces are shown with the mean drawn as a continuous line and SDs drawn as dotted lines in the same color on either side of the continuous line (Fig. 7). In each case, three to six experiments were performed (details in Fig. 7). There were five salient findings. (*i*) Remarkably, two of these five mutants, AGAR21 and -52, do not respond to chloroform. (*ii*) A xenon signal is present in W1118 and AGAR11, -52, and -211. (*iii*) An N_2O signal is present in HAR85 and AGAR11. (*iv*) The response of AGAR211 to $CHCl_3$ seems more transient than in WT flies. (*v*) The ion channel mutant HAR85 gives responses indistinguishable from WT controls. Equally remarkably, four of five AGAR mutants (AGAR11, -21, -52, and -53) were able to wake up after being exposed to four anesthetics in succession, unlike WT flies, which never recovered. These results strongly suggest a link between the pattern of changes in spin and anesthetic resistance in some of the AGAR mutants. It seems unlikely that it could be coincidental, because fly strains that do not exhibit anesthetic resistance, namely W1118, YW, and NRL (two experiments), have very similar anesthetic responses along with the channel mutant HAR85.

However, the correlation between anesthetic resistance and spin responses is clearly not perfect. Two lines (AGAR53 and -211) showed only small differences in their spin responses from the WT controls, and only AGAR53 flies woke up after the procedure. What is puzzling is that AGAR53 and -211 were also the most resistant to halothane anesthesia. The discrepancy could be because of the fact that the mutants were selected for their resistance to halothane and not to the chloroform used in our experiments. Indeed, AGAR211 did not, in fact, revive after chloroform. It could also be that different loci are involved, and only some of them work through an electronic mechanism. As it happens, AGAR53 and -211 were the best-characterized mutants, in which the gene locus had been mapped with some precision.

The perturbation of an electronic signal by Xe and SF_6 is, in itself, a surprising finding from a physicochemical point of view. Neither has a notably high electron affinity: xenon is, of course, totally inert under all but the most extreme chemical conditions, and SF_6 is sufficiently inert under ordinary conditions and used as a harmless tracer gas for underground rivers and a dielectric in high-voltage circuit breakers. The fact that these two gases are

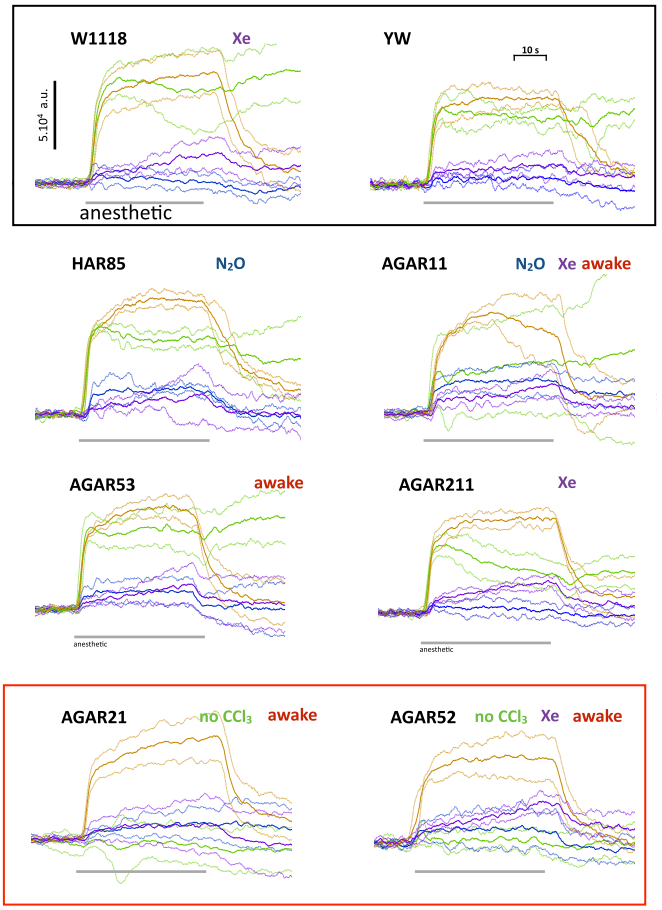

Fig. 7. Responses of eight different fly strains to the anesthetics. Each experiment involved exposure of the flies to Xe, SF_6, N_2O, and $CHCl_3$ in that order at ~3-min intervals. At the beginning and end of each experiment, a magnetic field scan was performed. The value of the magnetic field during anesthetic exposure was set at the first scan to the peak of the resonance (usually 3,345 G). Each figure shows the effects of the four anesthetics on a particular strain measured in the course of several (three to six) experiments. To give a visual estimate of the variability of the data, the mean (bold traces) and SDs (light dotted traces in the same color on either side of the mean trace) of the records obtained in each experiment are shown. We define the presence of a signal as when the mean deviates by more than 2 SDs from the zero line. For each strain, in addition to the obvious signals (SF_6-$CHCl_3$), we indicate (*Right*, row 1) which of the other anesthetics gave a response and whether the flies revived when placed in a Petri dish at room temperature after the experiments. W1118 WT (four experiments): SF_6 and $CHCl_3$ of comparable amplitude. SF_6 signal rises during exposure, and $CHCl_3$ decays slightly. On return to nitrogen, the SF_6 signal returns to baseline, and $CHCl_3$ signal remains close to peak. A gradually rising Xe signal is also present. YW (three experiments): very similar in amplitude and time course to W1118. HAR85 (three experiments): SF_6 signal was somewhat larger than $CHCl_3$, and there was a definite N_2O signal. AGAR11 (four experiments): SF_6 signal was normal, average $CHCl_3$ signal seems to be smaller but highly variable, and there are definite Xe and N_2O signals. Flies revive at end of experiment. AGAR21 (six experiments): SF_6 signal was normal, $CHCl_3$ signal was absent, and there were hints of Xe and N_2O signals that were not statistically significant. Flies revive at end of experiment. AGAR52 (four experiments): SF_6 signal was normal, $CHCl_3$ signal was absent, and there was a large Xe signal. Flies revive at end of experiment. AGAR53 (four experiments): signals were similar to HAR85, but there was no N_2O signal. Flies revive at end of experiment. AGAR211 (four experiments): SF_6 signal was normal, $CHCl_3$ decays during exposure, and there was a definite Xe signal.

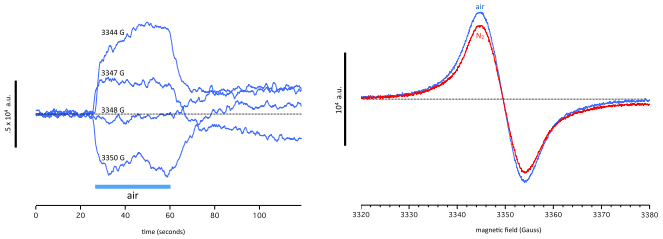

Fig. 8. (*Left*) The spin response when passing from N_2 to air at four different values of magnetic field indicated for each trace. The signal reverses sign when going from 3,344 to 3,350 G. (*Right*) Magnetic field scans performed on the same preparation in nitrogen (red trace) and air (blue trace), showing that the effect of air on the ESR resonance mirrors its behavior at fixed values of magnetic field.

able to affect an electron current is truly remarkable and fits in with the perturbations in electronic structure described in *Electronic Structure of Peptide–Volatile Agent Interactions*. Furthermore, the time course of the Xe effect seems to differ from the others, gradually rising during exposure. Given that Xe and SF_6 are of similar size, shape, and hydrophobicity and therefore, presumably diffuse similarly, this difference suggests that Xe acts in a different location.

Dioxygen signal, interactions between anesthetics, and CO_2. We noticed that going from N_2 to air caused an increase in spin of similar amplitude and time course as going from N_2 to SF_6. Applying the same method as we did to the SF_6 signal in *Anesthetic-induced spin change is a resonance*, we measured the response to air at different values of magnetic field. They are shown in Fig. 8. The signal is positive at 3,344 G, near zero at 3,348 G, and negative at 3,350 G. Scans of magnetic fields performed in N_2 and air show a difference in spin consistent with this behavior, with the curves crossing each other close to the cross-over point at 3,348 G.

We surmise, although this notion needs checking by additional experiments, that the effect of air is because of dioxygen rather than the decrease in N_2 partial pressure or the presence in air of other trace gases not present in pure N_2. This dioxygen signal is similar in amplitude, time course, and magnetic field dependence to the SF_6 signal. It cannot be caused by intrinsic paramagnetism of dioxygen, because the triplet signal from dioxygen is smeared by the proximity between the two unpaired spins and is much broader than the resonance that we observe. There is, however, a significant difference between the dioxygen and the anesthetic signals that emerged during experiments involving exposure to chloroform. In WT flies, the effect of chloroform is essentially irreversible over a scale of tens of minutes. After exposure to chloroform, the response to SF_6 is diminished in amplitude by about one-half (Fig. 9). By contrast, the response to dioxygen is less affected by chloroform and in some experiments, not at all, suggesting that the dioxygen response differs in some way from the anesthetic response. Interestingly, a synergy between oxygen and anesthetic gases in *Drosophila* has previously been reported (66).

CO_2 was used throughout these experiments to immobilize the flies, which is common practice when handling *Drosophila*. The effect of CO_2 is rapid and rapidly reversible, usually within 15 s after a brief exposure. The consensus seems to be that CO_2 is not a proper anesthetic (67). Our spin signal measurements concur with this notion: no effect of CO_2 on spin is seen in either fixed field or variable field measurements. Considering that the intracellular pH of every cell in the animal falls by ∼1 pH unit during 100% CO_2 exposure (68), it is remarkable that has no influence at all on either signal (Fig. 9).

Electronic Structure of Peptide–Volatile Agent Interactions. ***Anesthetics.*** When adsorbed on a metal surface, xenon and other GAs extend the Fermi sea by a bump surrounding the anesthetic molecule. This bump is made visible by STM measurements. As mentioned in the Introduction, the motivation for the experiments described above was the hunch that GAs might do the same to proteins. The nonmetallic analog of the Fermi level is the HOMO. We, therefore, used DFT calculations to see whether anesthetics perturb the HOMO of a model protein. DFT calculation times scale steeply with numbers of electrons; we, therefore, tried to keep the system small. The protein is represented by an α-helix of glycine residues. The choice of glycine (side chain: H) is biologically somewhat unrealistic, because a real α-helix composed entirely of glycine residues would not be structurally stable. The advantage of glycine from our point of view is that it enables a close approach of the anesthetic to the HOMO, which will be centered on a peptide bond in the helix backbone. To avoid end effects associated with the carboxylate group, the helix is terminated at both ends by a methyl group replacing the next α-carbon.

Preliminary calculations showed that there was little to be gained in terms of accuracy of HOMO calculations by extending the helix beyond nine residues. Accordingly, we took as our reference protein a nine-residue glycine helix optimized by DFT (PBE functional and TZP basis set) in vacuum. In subsequent computations, the coordinates of the helix atoms were held fixed, because the interactions that interest us are sufficiently weak that they would not be expected to greatly perturb the structure of the helix itself. (For the HOMO of the naked helix, see Fig. 11, column 1, row 1.) It is at the carboxyl end of the helix. When two identical helices are brought within a few angstroms of each other with their axes forming a right angle, the HOMO of the system is confined to one side because of minor asymmetries in the system. As expected, the HOMO-1 is on the other side and just 8 meV lower in energy. A xenon atom is inserted in the space

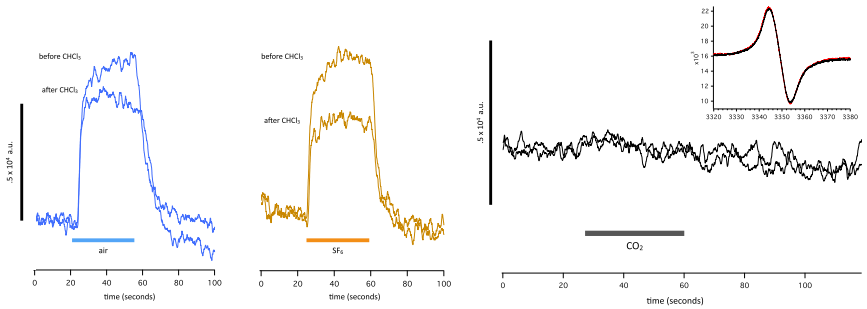

Fig. 9. Responses to (*Left*) air (blue) and (*Center*) SF_6 (brown) before and after a brief exposure to chloroform. The time elapsed before the first and second traces is 5 min. The SF_6 response is markedly reduced by exposure to chloroform, whereas the signal caused by air is less affected. (*Right*) Lack of effect of CO_2 on spin in either continuous measurement at a fixed field value or a magnetic field scan (*Inset*).

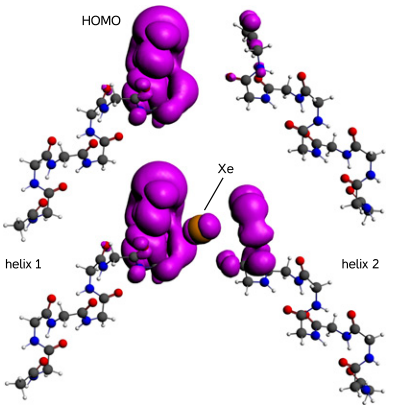

Fig. 10. The HOMO (purple surface; electron density = 0.003 e/Å^3) of two α-helices composed of nine glycine residues each. (*Upper*) When the gap is empty, the HOMO is almost confined to the left-hand helix. (*Lower*) When a xenon atom is present between the helices, the HOMO spreads from one helix to the other through the xenon atom. Orbital volume on the right-hand helix increases 3.9-fold from 15.3 to 60 Å^3.

between the fixed helices in the position optimized for a single helix (see Fig. 11) using a dispersion-corrected functional (PBE-D3). The dispersion correction introduces a small attractive force between helix and Xe, which causes the Xe to move closer to the helix until repulsive forces stop it. After optimization, the protein–Xe complex was recalculated at that geometry using the B3LYP functional, which reduces the electron self-interaction, to achieve a realistic spread of orbitals. The results are shown in Fig. 10 with and without the Xe atom. When Xe is absent, the HOMO barely extends across the gap. When Xe is present, the HOMO is greatly extended, and the HOMO volume on the right-hand helix increases nearly fourfold.

Xenon is easy to model because of its spherical symmetry. No docking is needed, and the relative orientation of the helices makes very little difference to HOMO spread. The other anesthetics are not spherically symmetric and would require docking to both helices. Docking would also require a variable interhelix space to accommodate anesthetics of various sizes. These seem like somewhat arbitrary choices in the absence of a known structure for the anesthetic binding site. However, because we expect the system to be symmetric in energy (i.e., donor and acceptor helices to have very close HOMO energies), we chose instead to calculate only one side of the bridge (i.e., omitting the second helix). The anesthetic was positioned along the helix axis a few angstrom away from the helix and allowed to relax without docking to its equilibrium position, where dispersion and repulsion forces balance each other. The results are shown in Fig. 11. There were five salient features. (*i*) Xenon and all anesthetic molecules perturb to a greater or lesser extent the HOMO of the nine-residue helix. (*ii*) Xenon and all anesthetic molecules extend the α-helix HOMO into the anesthetic itself. To get a better quantitative understanding of this effect, the added HOMO volume was calculated by subtracting from the volume of the HOMO with anesthetic that of the HOMO of the helix alone. To compensate for the fact that larger anesthetics have larger HOMOs, the added volume was divided by the molecular volume of the anesthetic itself. The resulting ratio (R) is shown above each helix–anesthetic combination in Fig. 11. (*iii*) The biggest perturbations and extensions are seen with barbital (R = 0.55), ether (R = 0.47), xenon (R = 0.33), alfaxalone (R = 0.25), etomidate (R = 0.20), and cyclopropane (R = 0.11). (*iv*) Remarkably, the nonanesthetic (convulsant) ether derivative fluothyl [bis(2,2,2)trifluoroethylether; R = 0.05] and 1,1,2,3,3,4-hexafluoro-2,4-dimethylcyclobutane (DMFPC; R = 0.03) (15) both had lower R values than their nonhalogenated counterparts. The orbital spread is not dependent on the dielectric constant of the medium surrounding the helix–anesthetic complex. Solvation in benzene and water using the Conductor Screening Model method (69) implemented in ADF does not alter the orbitals. (*v*) SF_6, although clearly causing some HOMO spread, has a low R value and does not quantitatively fit this relationship.

Nonanesthetics. The fact that HOMO spread in the two nonanesthetics fluothyl [bis(2,2,2)trifluoroethylether] and DMFPC is more limited than in related nonhalogenated molecules is encouraging. However, these calculations raise the question of what might be an appropriate nonanesthetic molecule to compare anesthetics with in electronic structure calculations. If one broadens the search from anesthesia to the older denomination of narcosis, it becomes clear that a vast range of substances, while not potent enough to cause outright unconsciousness, nevertheless have effects on the CNS that are reminiscent of

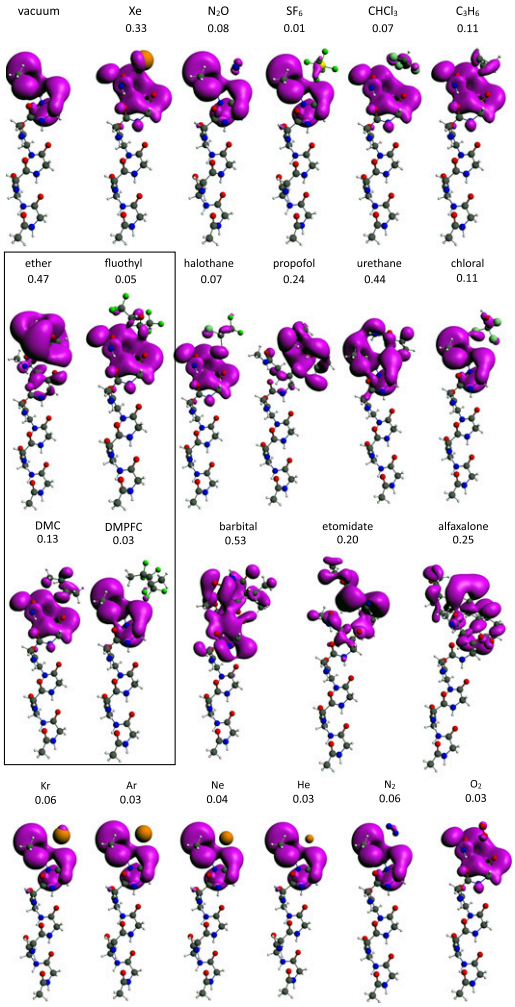

Fig. 11. Electronic structure of α-helix anesthetic complexes calculated by DFT (*Methods*). The HOMO is shown in purple. The number below each chemical name is the ratio of HOMO volume added by the anesthetic to the molecular volume of the anesthetic itself. The box contains two pairs of nonanesthetic halogenated and hydrogen counterparts for direct comparison of R values. Row 4 depicts gases relevant to diving physiology. Details are in the text. Alfaxalone, 3-hydroxypregnane-11,20-dione; barbital, 5,5-diethylpyrimidine-2,4,6(1H,3H,5H)-trione; chloral:trichloroethanal;halothane, 2-bromo-2-chloro-1,1,1-trifluoroethane; ether, diethyl ether; etomidate, ethyl 3-[(1R)-1-phenylethyl]imidazole-5-carboxylate; fluothyl, bis(2,2,2-trifluoroethyl) ether; propofol, 2,6-diisopropylphenol; urethane, ethyl carbamate. DMC, dimethylcyclobutane.

light stages of anesthesia. Inhalants commonly abused for their CNS effects (70) include alkanes, like propane and butane, and aromatics, like toluene, etc. Indeed, alkanes, like dimethylcyclobutane, show some degree of orbital spread. It is not surprising that such a general mechanism as the one that we propose should be found to a greater or lesser extent in molecules beyond those in clinical anesthesia proper.

One interesting class of gases of great practical importance is the component gases of air and substitutes for air in hyperbaric conditions, such as the lighter noble gases. Pure oxygen and nitrogen cause convulsions (71) and a narcosis (72) very similar to that caused by nitrous oxide at 12- (oxygen) and ∼40-m (nitrogen) depth, respectively. Indeed, it has been shown that nitrogen, even in its normal proportion in air at atmospheric pressure, causes a slight but detectable narcosis, which is revealed when subjects breathe helium and oxygen instead (73). At high pressures, helium has proven to be the gas of choice for diving; close to atmospheric pressure, helium and neon seem completely devoid of anesthetic action (74), whereas argon and krypton are slightly anesthetic (12, 39). It, therefore, seems interesting to ask whether these properties are mirrored in their electronic structure. This is partially the case, which is shown in Fig. 11, row 4. Krypton has the highest R value of the series at 0.06, similar to that of nitrogen, whereas the other noble gases have lower R values. Dioxygen (triplet state) has a low R value but perturbs the shape of the helix HOMO, perhaps coincidentally, in a way remarkably similar to that of the convulsant fluothyl.

Discussion

Origin of the Spin Signal. The central question raised by these results is what species carries the anesthetic-induced increase in spin. Changes in paramagnetism, such as the ones that we observed, could, in principle, be caused by a change in spin in a chemical species. The chemical species could be either an organic molecule accepting an electron to form a radical anion or a transition metal undergoing a redox reaction. Organic radicals seem unlikely: as described in *SF_6-dependent spin signal requires cell integrity*, a typical SF_6 signal of 7,000 units, therefore, represents an increase in spins in the cavity of the order of 2.8×10^{13} spins. Given that the chamber contains an average of 30 flies, each weighing ∼1 mg, this amount of spin would translate into an organic free radical concentration of ∼1.5 μM, which is orders of magnitude larger than anything seen in 60 y of biological ESR (75). By contrast, a change in the redox state of a metal is not implausible. Cu and Fe are present in sufficient amounts in *Drosophila* (220 and 52 μM, respectively) to be able, in principle, to exhibit such spin changes. [We thank Nikolaos S. Thomaidis (University of Athens, Athens, Greece) for these measurements.] Note, however, that most of the Cu will be bound to the insect blood pigment, hemocyanin, in a diamagnetic state (76) and will not contribute to the signal. As a simple check for changes in the redox state of iron, we looked for a signal at $g \sim 4.0$ (typical of high-spin iron in complexes) (77) and found none. This observation does not rule out other spin states of iron and copper, although the line width would seem to be unusually narrow for a metal ion (78).

Another possibility is that we are looking at electrons in melanin, the prevalent stable free radical. The signal is strikingly similar in shape to that of melanin and seems indistinguishable from what would happen if melanin spin increased during anesthesia. However, it cannot be caused by eumelanin, because the signal is unchanged in yellow and neuralized flies. It is conceivable that anesthetics perturb the concentrations of charge carriers in the remainder of the melanins (i.e., pheo- and neuromelanins). Similar effects of gases—although apparently not xenon—are seen and put to work in conducting polymers and semiconductor gas sensors (79). However, it is hard to see how a melanin signal could account for all these observations. First, the effect would have to be specific to pheo- and neuromelanins, despite their structural similarities with eumelanins. Second, mutations would have to suppress the response of pheo- and neuromelanins to one anesthetic (chloroform) but not the another anesthetic (SF_6). It seems unlikely that such random polymers could be affected in this fashion. Third, the fact that cell integrity is required for a full-amplitude, steady-state signal suggests that the anesthetics do not act directly on a spin-containing substance such as melanin but instead, require organelles to generate an electron current. Nevertheless, the possibility that neuromelanins may be involved cannot be ruled out: they are the gray in gray matter (80), and their role has not been elucidated.

The specific effect of mutations on the anesthetic responses is, instead, suggestive of a protein. What then would the charge carriers be? Proteins are generally thought to be good insulators, with a band gap of the order of 5 eV. However, Pethig and Szent-Györgyi (81) have described hole conduction in casein covalently bound to pyruvic aldehyde. Pyruvic aldehyde (a side product of metabolism) forms a Schiff base with lysines. The high electron affinity of the Schiff bases imine and iminium creates an acceptor impurity, which in turn, creates holes and allows electronic conduction. The modified protein is an electronic conductor and gives an ESR signal comparable with our ESR signal. It has recently become clear that the chemistry described by Pethig and Szent-Györgyi (81) occurs in living systems (82). Indeed, many compounds, both pharmacological and physiological, have sufficient electron affinity to create electron holes in proteins (83). If electrons are, indeed, moving inside proteins, then the resemblance in amplitude and time course between the SF_6 signal and the dioxygen signal may be significant. From an ESR standpoint, the main difference between flies in air and flies in nitrogen will be the electron current flowing through the electron transport chain of mitochondria. Dioxygen consumption in *Drosophila* at 26 °C amounts to $\sim 2.4 \times 10^{-11}$ M/s or ∼10 μA electron current per fly, allowing for the fact that four electrons reduce one dioxygen molecule (84). These numbers are, at any rate, comparable with the size of the signals that we observe, even accounting for the severalfold reduction in metabolism caused by the 6 °C temperature in the ESR chamber. In both the redox and the carrier mechanisms, there may be many gaps that are bridged by the anesthetic in different locations and different circuits. In this sense, what we propose is a theory that is unitary in mechanism but not in location.

An alternative possibility is that the change in observed spin is not caused by a change in the total spin content of the preparation but instead, caused by a change in spin polarization. It has recently been shown that electrons traversing chiral materials can become spin-polarized in the direction of motion (85, 86). This spin polarization can reach 80% in thin layers of some biological materials, and even higher values may occur when electrons can interact with chiral materials over longer distances. The intensity of an ESR resonance depends very sensitively on the distribution between spin-up and spin-down states, normally governed by a Boltzmann equilibrium. A perturbation of that equilibrium by a change in electronic structure could, in principle, cause changes in the ESR signal while keeping total unpaired electron number constant. Additional experiments are needed to determine which of these mechanisms can account for the anesthetic signal.

Connection Between Electrons and Anesthesia. Our electronic structure calculations fall far short of a quantitative analysis, partly because the structure of the anesthetic binding site is unknown. Our purpose in this paper was to explore the possibility that, qualitatively, all GAs can extend protein HOMOs. This seems to be the case. The calculated R value seems to give a good heuristic for anesthetic action and correctly predicts the high anesthetic potencies of Xe, barbital, etomidate, alfaxalone,

and cyclopropane and the nonanesthetic nature of fluothyl and DMFPC. SF_6 is clearly anomalous, maybe because DFT methods, although generally accurate when calculating HOMO energies (87), are known to miscalculate SF_6 by several electronvolts (88). The other results are in general agreement with the Meyer–Overton relationship and its best-documented exceptions. Because the HOMO resides in the amide backbone, these results are likely to have some generality, insofar as all proteins will have similar amide HOMO energies, regardless of side chains. If correct, therefore, this effect on electronic structure is likely to be a general phenomenon, consistent with the fact that GAs act on all animal species on which they have been tested.

The significance of these results will, therefore, depend largely on their applicability to other organisms, because it is very unlikely that different mechanisms will account for anesthesia in different species. Anesthetic-resistant mutants have been described in mice, *Caenorhabditis elegans*, and even yeast (89). If, say, organisms as remote in evolution as mice and *C. elegans* show the same effects as flies, there is a chance that the mechanism of GA may be on its way to elucidation. The advantage of these preparations over *Drosophila* is that one would no longer be confined to volatile anesthetics. Mice could be injected with and yeast and nematodes could be exposed to the full range of GAs, including those with little or no vapor pressure. The difficulty will reside in overcoming the practical limit to X-band measurements of ~50 mg water in the RF cavity. It also remains to be seen if L-band spectrometers, which tolerate larger amounts of tissue, are sufficiently sensitive to detect these signals. In additional experiments planned on *Drosophila*, electron-nuclear double resonance and pulsed ESR would also likely help identify the paramagnetic species. Freezing preparations to cryogenic temperatures in the presence of various anesthetics may also improve resolution.

Why then should the electronic conductance of GAs matter to neurons, because the electrical currents that set neurons apart from inexcitable cells are carried by ions and not by electrons? It is tempting to speculate as to what answers to this question might emerge from an understanding of the genes involved. We can think of several possibilities (in increasing order of interest and remoteness). (*i*) The spin change could turn out to be linked to electron currents in mitochondria. Links between GAs and electron transport are already well-known: the barbiturate Amytal perturbs electron transport in mitochondria (90), and many other effects of GAs on electron function have been reported (91, 92). However, GAs cannot act solely through mitochondria, because mitochondrial blockers uncouplers, although toxic, are not anesthetic (93, 94). (*ii*) It could be caused by redox reactions, where electrons are used to break a chemical bond (for example, a disulfide). This electrochemical effect would be similar to an electronic mechanism proposed for receptors mediating olfactory transduction (95). Disulfide redox reactions have been shown to be important in modulation of the $GABA_A$ receptor (96, 97), which is implicated in the action of many anesthetics. (*iii*) An interesting variation is that the electron current could flow to remote parts of the cell through an unknown current pathway—the cytoskeleton is an obvious candidate—to control proteins at the end of the wire without incurring diffusion delays. (*iv*) The electrons may, thus, be used to write a bit of memory, by either as above, electroreduction of a disulfide or redox action on a metal ion. (*v*) Lastly, the electron currents could be used to perform logical operations and computation. The connection of these hypothetical mechanisms to CNS physiology remains to be determined.

Conclusion. In summary, (*i*) the electron spin changes that we measure are related to anesthesia insofar as they differ in anesthesia-resistant mutants. (*ii*) The perturbations to electronic structure of a protein model seem able to account, at least qualitatively, for both the Meyer–Overton relationship and some well-documented exceptions to it. (*iii*) We propose that the two are related. Our results establish a possible link between (un) consciousness in flies and electron currents detectable by a change in a quantum observable, electron spin.

ACKNOWLEDGMENTS. We thank Maria Anezaki, Katerina Papanikolopoulou, and Klio Maniati for assistance with *Drosophila*; K. S. Krishnan for supplying us with the autosomal gene anesthetic-resistant mutants; and Misha Perouansky, Peter Hore, Gareth Eaton, Susana Huelga, and Alberto Lesarri for useful comments. Stan van Gisbergen and Olivier Visser at SCM are thanked for assistance with the ADF code. Adani Ltd is thanked for assistance with the ESR spectrometer. This work was supported by US Defense Advanced Research Projects Agency Grant N66001-10-1-4062.

1. Perouansky M (2012) The quest for a unified model of anesthetic action: A century in Claude Bernard's shadow. *Anesthesiology* 117(3):465–474.
2. Oliver AE, Deamer DW, Akeson M (1991) Evidence that sensitivity to steroid anesthetics appears late in evolution. *Brain Res* 557(1-2):298–302.
3. Zimmerman PW, Hitchcock AE, Crocker W (1936) Unsaturated carbon gases as plant stimulants and anesthetics. *Anesth Analg* 15(1):5–9.
4. Okazaki N, Takai K, Sato T (1993) Immobilization of a sensitive plant, Mimosa pudica L., by volatile anesthetics. *Masui* 42(8):1190–1193.
5. De Luccia TP (2012) Mimosa pudica, Dionaea muscipula and anesthetics. *Plant Signal Behav* 7(9):1163–1167.
6. Kennedy D, Norman C (2005) What don't we know? *Science* 309(5731):75.
7. Alkire MT, Hudetz AG, Tononi G (2008) Consciousness and anesthesia. *Science* 322(5903):876–880.
8. Kulli J, Koch C (1991) Does anesthesia cause loss of consciousness? *Trends Neurosci* 14(1):6–10.
9. Hameroff SR (2006) The entwined mysteries of anesthesia and consciousness: Is there a common underlying mechanism? *Anesthesiology* 105(2):400–412.
10. Albert A (1985) *Selective Toxicity: The Physico-Chemical Basis of Therapy* (Chapman & Hall, London).
11. Lawrence JH, Loomis WF, Tobias CA, Turpin FH (1946) Preliminary observations on the narcotic effect of xenon with a review of values for solubilities of gases in water and oils. *J Physiol* 105:197–204.
12. Cullen SC, Gross EG (1951) The anesthetic properties of xenon in animals and human beings, with additional observations on krypton. *Science* 113(2942):580–582.
13. Laubach GD, P'an SY, Rudel HW (1955) Steroid anesthetic agent. *Science* 122(3158):78.
14. James R, Glen JB (1980) Synthesis, biological evaluation, and preliminary structure-activity considerations of a series of alkylphenols as intravenous anesthetic agents. *J Med Chem* 23(12):1350–1357.
15. Koblin DD, et al. (1994) Polyhalogenated and perfluorinated compounds that disobey the Meyer-Overton hypothesis. *Anesth Analg* 79(6):1043–1048.
16. Meyer H (1899) Welche Eigenschaft der Anasthetica bedingt ihre narkotische Wirkung? *Naunyn Schmiedebergs Arch Exp Pathol Pharmakol* 42:109–118.
17. Overton E (1901) *Studien über die Narkose* (Fischer, Stuttgart).
18. Cantor RS (1997) The lateral pressure profile in membranes: A physical mechanism of general anesthesia. *Biochemistry* 36(9):2339–2344.
19. Mullins LJ (1954) Some physical mechanisms in narcosis. *Chem Rev* 54(2):289–323.
20. Seeman P (1972) The membrane actions of anesthetics and tranquilizers. *Pharmacol Rev* 24(4):583–655.
21. Miller KW, Paton WD, Smith RA, Smith EB (1973) The pressure reversal of general anesthesia and the critical volume hypothesis. *Mol Pharmacol* 9(2):131–143.
22. Lee AG (1976) Interactions between anesthetics and lipid mixtures. Normal alcohols. *Biochemistry* 15(11):2448–2454.
23. Trudell JR (1977) A unitary theory of anesthesia based on lateral phase separations in nerve membranes [proceedings]. *Biophys J* 18(3):358–359.
24. Gruner SM, Shyamsunder E (1991) Is the mechanism of general anesthesia related to lipid membrane spontaneous curvature? *Ann N Y Acad Sci* 625:685–697.
25. Burn JH, Epstein HG (1946) Theories of anaesthetic action. *BMJ* 2(4475):533.
26. Featherstone RM, Muehlbaecher CA, Debon FL, Forsaith JA (1961) Interactions of inert anesthetic gases with proteins. *Anesthesiology* 22:977–981.
27. Pauling L (1964) The hydrate microcrystal theory of general anesthesia. *Anesth Analg* 43:1–10.
28. Bangham AD, Mason WT (1980) Anesthetics may act by collapsing pH gradients. *Anesthesiology* 53(2):135–141.
29. Chiou JS, Ma SM, Kamaya H, Ueda I (1990) Anesthesia cutoff phenomenon: Interfacial hydrogen bonding. *Science* 248(4955):583–585.
30. Brockerhoff H, Zingoni J, Brockerhoff S (1990) Mechanism of anesthesia: Anesthetics may restructure the hydrogen belts of membranes. *Neurochem Int* 17(1):15–19.
31. Qin Z, Szabo G, Cafiso DS (1995) Anesthetics reduce the magnitude of the membrane dipole potential. Measurements in lipid vesicles using voltage-sensitive spin probes. *Biochemistry* 34(16):5536–5543.

32. Ueda I (1965) Effects of diethyl ether and halothane on firefly luciferin bioluminescence. *Anesthesiology* 26:603–606.
33. Franks NP, Lieb WR (1978) Where do general anaesthetics act? *Nature* 274(5669): 339–342.
34. Moss GW, Lieb WR, Franks NP (1991) Anesthetic inhibition of firefly luciferase, a protein model for general anesthesia, does not exhibit pressure reversal. *Biophys J* 60(6):1309–1314.
35. Franks NP, Lieb WR (1991) Stereospecific effects of inhalational general anesthetic optical isomers on nerve ion channels. *Science* 254(5030):427–430.
36. Hall AC, Lieb WR, Franks NP (1994) Stereoselective and non-stereoselective actions of isoflurane on the GABAA receptor. *Br J Pharmacol* 112(3):906–910.
37. Franks NP, Lieb WR (1997) Selectivity of general anesthetics: A new dimension. *Nat Med* 3(4):377–378.
38. Franks NP, Dickinson R, de Sousa SL, Hall AC, Lieb WR (1998) How does xenon produce anaesthesia? *Nature* 396(6709):324.
39. Trudell JR, Koblin DD, Eger EI, 2nd (1998) A molecular description of how noble gases and nitrogen bind to a model site of anesthetic action. *Anesth Analg* 87(2):411–418.
40. Eckenhoff RG, Johansson JS (1997) Molecular interactions between inhaled anesthetics and proteins. *Pharmacol Rev* 49(4):343–367.
41. Eckenhoff RG (2008) Why can all of biology be anesthetized? *Anesth Analg* 107(3): 859–861.
42. Sonner JM, Cantor RS (2013) Molecular mechanisms of drug action: An emerging view. *Annu Rev Biophys* 42:143–167.
43. Bhattacharya AA, Curry S, Franks NP (2000) Binding of the general anesthetics propofol and halothane to human serum albumin. High resolution crystal structures. *J Biol Chem* 275(49):38731–38738.
44. Sauguet L, et al. (2013) Structural basis for potentiation by alcohols and anaesthetics in a ligand-gated ion channel. *Nat Commun* 4:1697.
45. Eigler DM, Schweizer EK (1990) Positioning single atoms with a scanning tunnelling microscope. *Nature* 344:524–526.
46. Eigler DM, Weiss PS, Schweizer EK, Lang ND (1991) Imaging Xe with a low-temperature scanning tunneling microscope. *Phys Rev Lett* 66(9):1189–1192.
47. Watanabe K, et al. (2005) Orientation of nitrous oxide on palladium (110) by STM. *Chem Phys Lett* 406(4-6):474–478.
48. Sakamaki K, Matsunaga S, Itoh K, Fujishima A, Gohshi Y (1989) Imaging the phenol molecule adsorbed on TiO< sub> 2(110) by scanning tunneling microscopy. *Surf Sci* 219(3):L531–L536.
49. Nishino T, Bühlmann P, Ito T, Umezawa Y (2001) Scanning tunneling microscopy with chemically modified tips: Orientation-sensitive observation of ether oxygens. *Surf Sci* 490(1-2):L579–L584.
50. Yau S-L, Kim Y-G, Itaya K (1996) In situ scanning tunneling microscopy of benzene adsorbed on Rh (111) and Pt (111) in HF solution. *J Am Chem Soc* 118(33):7795–7803.
51. Takeuchi H, Kawauchi S, Ikai A (1996) Differentiation of chemically functional groups in stearoyl amide and anilide with scanning tunneling microscopy. *Jpn J Appl Phys* 35(Part 1, no. 6B):3754–3758.
52. Kim J-T, Kawai T, Yoshinobu J, Kawai M (1996) Adsorption of pyrimidine molecules on Pd (110) observed by scanning tunneling microscopy. *Surf Sci* 360(1-3):50–54.
53. Acevedo SF, Tsigkari KK, Grammenoudi S, Skoulakis EM (2007) In vivo functional specificity and homeostasis of Drosophila 14-3-3 proteins. *Genetics* 177(1):239–253.
54. Eaton GR, Eaton SS, Barr DP, Weber RT (2010) *Quantitative EPR* (Springer, Wien, New York).
55. Swartz HM, Bolton JR, Borg DC (1972) *Biological Applications of Electron Spin Resonance* (Wiley Interscience, New York).
56. Blois MS, Zahlan AB, Maling JE (1964) Electron spin resonance studies on melanin. *Biophys J* 4:471–490.
57. Trapp C, Waters B, Lebendiger G, Perkins M (1983) Electron spin resonances of a living system (Drosophila) on normal and carcinogenic diets. *Biochem Biophys Res Commun* 112(2):602–605.
58. Grabski AC (2009) Advances in preparation of biological extracts for protein purification. *Methods Enzymol* 463:285–303.
59. Haddad GG, Wyman RJ, Mohsenin A, Sun Y, Krishnan SN (1997) Behavioral and electrophysiologic responses of Drosophila melanogaster to prolonged periods of anoxia. *J Insect Physiol* 43(3):203–210.
60. Lesarri A, Vega-Toribio A, Suenram RD, Brugh DJ, Grabow J-U (2010) The conformational landscape of the volatile anesthetic sevoflurane. *Phys Chem Phys* 12(33): 9624–9631.
61. Krishnan KS, Nash HA (1990) A genetic study of the anesthetic response: Mutants of Drosophila melanogaster altered in sensitivity to halothane. *Proc Natl Acad Sci USA* 87(21):8632–8636.
62. Campbell DB, Nash HA (1994) Use of Drosophila mutants to distinguish among volatile general anesthetics. *Proc Natl Acad Sci USA* 91(6):2135–2139.
63. Mir B, Iyer S, Ramaswami M, Krishnan KS (1997) A genetic and mosaic analysis of a locus involved in the anesthesia response of Drosophila melanogaster. *Genetics* 147(2):701–712.
64. Madhavan MC, Kumar RA, Krishnan KS (2000) Genetics of anesthetic response: Autosomal mutations that render Drosophila resistant to halothane. *Pharmacol Biochem Behav* 67(4):749–757.
65. Nash HA, Scott RL, Lear BC, Allada R (2002) An unusual cation channel mediates photic control of locomotion in Drosophila. *Curr Biol* 12(24):2152–2158.
66. Fenn WO (1967) Interactions of oxygen and inert gases in Drosophila. *Respir Physiol* 3(2):117–129.
67. Caroll GC, Rothenberg DM (1992) Carbon dioxide narcosis. Pathological or "pathillogical"? *Chest* 102(4):986–988.
68. Turin L, Warner AE (1980) Intracellular pH in early Xenopus embryos: Its effect on current flow between blastomeres. *J Physiol* 300:489–504.
69. Klamt A, Schüürmann G (1993) COSMO: A new approach to dielectric screening in solvents with explicit expressions for the screening energy and its gradient. *J Chem Soc Perkin 1* 2:799–805.
70. Balster RL (1998) Neural basis of inhalant abuse. *Drug Alcohol Depend* 51(1-2): 207–214.
71. Yarbrough OD, Welham W, Brinton ES, Behnke AR (1947) *Symptoms of Oxygen Poisoning and Limits of Tolerance at Rest and at Work*. Available at http://archive.rubicon-foundation.org/3316.
72. Baddeley AD, De Figueredo JW, Curtis JW, Williams AN (1968) Nitrogen narcosis and performance under water. *Ergonomics* 11(2):157–164.
73. Winter PM, Bruce DL, Bach MJ, Jay GW, Eger EI, 2nd (1975) The anesthetic effect of air at atmospheric pressure. *Anesthesiology* 42(6):658–661.
74. Koblin DD, et al. (1998) Minimum alveolar concentrations of noble gases, nitrogen, and sulfur hexafluoride in rats: Helium and neon as nonimmobilizers (non-anesthetics). *Anesth Analg* 87(2):419–424.
75. Berliner LJ (2003) *In Vivo EPR (ESR): Theory and Application* (Kluwer, New York).
76. Moss TH, Gould DC, Ehrenberg A, Loehr JS, Mason HS (1973) Magnetic properties of Cancer magister hemocyanin. *Biochemistry* 12(13):2444–2449.
77. Shima T, et al. (1997) Binding of iron to neuromelanin of human substantia nigra and synthetic melanin: An electron paramagnetic resonance spectroscopy study. *Free Radic Biol Med* 23(1):110–119.
78. Carrington A, Luckhurst GR (1964) Electron spin resonance line widths of transition metal ions in solution. Relaxation through zero-field splitting. *Mol Phys* 8(2):125–132.
79. Kaur M, Aswal DK, Yakhmi JV, Gupta SK (2007) *Chemiresistor Gas Sensors: Materials, Mechanisms and Fabrication. Science and Technology of Chemiresistor Gas Sensors*, eds Aswal DK, Gupta SK (Nova Science Publishers, Inc., New York), pp 33–93.
80. Hearing VJ (2009) The expanding role and presence of neuromelanins in the human brain–why gray matter is gray. *Pigment Cell Melanoma Res* 22(1):10–11.
81. Pethig R, Szent-Györgyi A (1977) Electronic properties of the casein-methylglyoxal complex. *Proc Natl Acad Sci USA* 74(1):226–228.
82. Thornalley PJ, Langborg A, Minhas HS (1999) Formation of glyoxal, methylglyoxal and 3-deoxyglucosone in the glycation of proteins by glucose. *Biochem J* 344(Pt 1): 109–116.
83. Kovacic P, Somanathan R (2010) Mechanism of conjugated imine and iminium species, including marine alkaloids: Electron transfer, reactive oxygen species, therapeutics and toxicity. *Curr Bioact Compd* 6(1):46–59.
84. Kucera WG (1934) Oxygen consumption in the male and female fly, Drosophila melanogaster. *Physiol Zool* 7(3):449–458.
85. Naaman R, Waldeck DH (2012) Chiral-induced spin selectivity effect. *J Phys Chem Lett* 3(16):2178–2187.
86. Mishra D, et al. (2013) Spin-dependent electron transmission through bacteriorhodopsin embedded in purple membrane. *Proc Natl Acad Sci USA* 110(37):14872–14876.
87. Speelman AL, Gillmore JG (2008) Efficient computational methods for accurately predicting reduction potentials of organic molecules. *J Phys Chem A* 112(25): 5684–5690.
88. Chen ES, Chen EC (2014) Negative surface ionization electron affinities and activation energies of SF(n). *Rapid Commun Mass Spectrom* 28(5):527–535.
89. Morgan PC, Sedensky MM (2010) Genetics and anesthetic mechanism. *Molecular Bases of Anesthesia*, eds Moody E, Skolnick P (CRC Press, Boca Raton, FL), p 95.
90. Kater JM (1935) Sodium amytal for anesthesia in studies on mitochondria. *Science* 82(2124):256.
91. Cohen PJ (1973) Effect of anesthetics on mitochondrial function. *Anesthesiology* 39(2):153–164.
92. Pshenichnyuk SA, Modelli A (2013) Can mitochondrial dysfunction be initiated by dissociative electron attachment to xenobiotics? *Phys Chem Phys* 15(23):9125–9135.
93. Way JL (1984) Cyanide intoxication and its mechanism of antagonism. *Annu Rev Pharmacol Toxicol* 24:451–481.
94. Miranda EJ, McIntyre IM, Parker DR, Gary RD, Logan BK (2006) Two deaths attributed to the use of 2,4-dinitrophenol. *J Anal Toxicol* 30(3):219–222.
95. Turin L (1996) A spectroscopic mechanism for primary olfactory reception. *Chem Senses* 21(6):773–791.
96. Pan Z-H, Bähring R, Grantyn R, Lipton SA (1995) Differential modulation by sulfhydryl redox agents and glutathione of GABA- and glycine-evoked currents in rat retinal ganglion cells. *J Neurosci* 15(2):1384–1391.
97. Amato A, Connolly CN, Moss SJ, Smart TG (1999) Modulation of neuronal and recombinant GABAA receptors by redox reagents. *J Physiol* 517(Pt 1):35–50.